A Study of Oxygen Vacancy Formation and Annihilation in Submonolayer Coverages of TiO_2 Dispersed on MCM-48†

Jennifer Strunk, William C. Vining, and Alexis T. Bell*

Department of Chemical Engineering, University of California, Berkeley, California 94720-1462 and Chemical Sciences Division, Lawrence Berkeley National Laboratory, Berkeley, California 94720

Received: January 5, 2010; Revised Manuscript Received: May 13, 2010

The reduction and reoxidation of submonolayer coverages of TiO_2 deposited onto MCM-48 were investigated. The deposited TiO_2 was characterized by Raman and UV−visible spectroscopy. Raman spectra show that Ti atoms are bonded to the silica support by Ti−O−Si bonds and that crystalline TiO_2 is not formed. The results of the Raman and UV−visible spectroscopy suggest that the dispersed TiO_2 is present as two-dimensional oligomeric structures. Reduction in H_2 at 923 K produces Ti^{3+} cations observable by EPR ($g = 1.932$), suggesting the formation of oxygen vacancies. The fraction of Ti that could be reduced increased with TiO_2 surface concentration. This observation is attributed to the ease with which O atoms can be removed from the TiO_2 overlayer as the size of the titania patches increases. The amount of oxygen removed during reduction was quantified by pulsed reoxidation. It was observed that the temperature required for complete reoxidation decreased with increasing surface coverage of the silica support by TiO_2. This trend is explained with a proposed model of the reoxidation process, in which the rate limiting step is the migration of peroxide species through or between the deposited TiO_2 patches. A linear correlation was established between the intensity of the EPR signal for Ti^{3+} and the amount of oxygen removed from TiO_2/SiO_2. This relationship was then used to determine the oxygen vacancy concentration present on the surface of TiO_2/SiO_2 after temperature-programmed oxidation of methanol.

Introduction

Crystalline anatase and rutile are good supports for both metal and metal oxide catalysts; however, such forms of TiO_2 are difficult to prepare with high surface area and have a tendency to sinter at low temperatures.[1−6] These shortcoming can be overcome by dispersing of TiO_2 on a high-surface-area support, such as mesoporous SiO_2.[7,8] By this means, the chemical properties of TiO_2 are combined with the high surface area and the high thermal stability of the SiO_2. Such TiO_2/SiO_2 materials exhibit catalytic activity and selectivity not possessed by bulk TiO_2. For example, TiO_2/SiO_2 is active for liquid-phase epoxidation of alkenes, whereas bulk TiO_2 is not.[1,2,9,10] Likewise, TiO_2/SiO_2 is active for the gas-phase oxidation of methanol to formaldehyde and methylformate, whereas bulk TiO_2 promotes the condensation of methanol to dimethyl ether.[3,11] TiO_2/SiO_2 has also been used as a support for dispersed vanadia,[12,13] and $VO_x/TiO_2/SiO_2$ has been shown to have a considerably higher activity for methanol oxidation to formaldehyde than VO_x/SiO_2.[14,15]

It is well-known that TiO_2 can lose oxygen, resulting in the formation of both bulk and surface vacancies.[1,16−23] The presence of such oxygen vacancies changes both the electronic and chemical properties of TiO_2 and, consequently, the performance of TiO_2 as both a catalyst and a catalyst support.[1,24−29] For example, oxygen vacancies have been shown to affect the photocatalytic activity of TiO_2,[30,31] the preferential adsorption of water and alcohols,[32,33] and the anchoring of noble metal clusters, such as gold[34,35] or platinum.[36] Oxygen vacancies on TiO_2 have also been suggested to increase the catalytic activity of gold[34,37] and copper[38] nanoparticles supported on TiO_2, and oxygen vacancies have been proposed to be responsible for the high activity of isolated vanadate species dispersed on TiO_2 for methanol oxidation to formaldehyde.[14,39]

Studies of oxygen vacancy formation in bulk TiO_2 suggest that surface vacancies are more stable than bulk vacancies and that vacancies can migrate from the bulk to the surface of the oxide.[40,41] However, only limited attempts have been made to quantify the surface concentration of O-atom defects. STM studies show that upon heating rutile in vacuum to 700−1100 K, the (110) surface of rutile can contain 2−10% O vacancies.[1,42−47] Vacancies are also formed in bulk TiO_2 powders by heating in vacuum or an inert atmosphere[48,49] or in a reducing gas.[50,51]

By contrast, nothing is known about the formation of vacancies in two-dimensional structures of TiO_2 formed on SiO_2. Given the differences in the structure of dispersed and bulk TiO_2, it is reasonable to expect that significant differences could exist between the two types of materials with regard to the formation and annihilation of anionic vacancies. For example, whereas Ti has a 6-fold coordination in anatase and rutile,[1] at low loading, Ti cations in the dispersed Ti species on SiO_2 are believed to be predominantly 4-fold-coordinated with increasing numbers of 5- and 6-coordinated Ti cations at higher coverages.[3,9] Silica-supported TiO_2 monolayers also lack the subsurface transition metal oxide, which can delocalize charge.

Oxygen vacancies in bulk TiO_2 can be detected using EPR spectroscopy because the electrons remaining in the vacancy move toward the neighboring Ti atoms forming two reduced Ti^{3+} cations,[39,52,53] according to

† Part of the "D. Wayne Goodman Festschrift".

* To whom correspondence should be addressed. E-mail: bell@cchem.berkeley.edu.

10.1021/jp100104d
Published on Web 06/11/2010

$$Ti^{4+}\text{-}O\text{-}Ti^{4+} \rightarrow Ti^{3+}\text{-}\square\text{-}Ti^{3+} + {}^1/_2O_2 \quad (1)$$

The presence of Ti^{3+} cations is also readily discernible by the blue color of partially reduced TiO_2.[16,54,55] In the current study, reduction−reoxidation studies in combination with EPR spectroscopy are used to investigate the reducibility of submonolayer coverages of TiO_2 dispersed onto MCM-48, a mesoporous silica, and the ease with which the oxygen vacancies can be removed. The maximum percentage of Ti atoms that can be reduced to the 3+ state is found to be a function of the Ti loading. The oxygen uptake varies with the reoxidation temperature because the oxygen vacancies are partially kinetically stable at temperatures below 473 K. The temperature needed for complete reoxidation of the TiO_2/SiO_2 samples decreases with increasing Ti loading. The results of this study suggest that the formation of oxygen vacancies is facilitated when the O atom to be removed is surrounded by a large number of Ti−O−Ti bonds. It is also shown that oxygen vacancies are not completely removed upon reoxidation in O_2 and can persist during methanol oxidation.

Experimental Section

Sample Synthesis and Characterization. The support used in the present studies, MCM-48, was prepared following the procedure given in ref 56. Submonolayer coverages of noncrystalline TiO_2 were dispersed onto the surface of the MCM-48 by grafting $Ti(O^iPr)_4$ from a solution of dry toluene.[14] MCM-48 support dried overnight at 393 K under vacuum was brought into contact with a solution of $Ti(O^iPr)_4$ dissolved in about 60 mL of dry toluene at room temperature under inert atmosphere. After stirring the solution with the support for 4 h, the solution was removed, and the sample was washed three times with ~60 mL of fresh toluene before it was dried overnight under vacuum at room temperature. The dried material was then heated to 573 K in helium and kept at this temperature for 1 h under synthetic air before it was heated in synthetic air to 773 K and kept at this temperature for 4 h. Following this procedure, Ti loadings of up to 1 Ti/nm^2 could be achieved. For Ti loadings higher than 1 Ti/nm^2, the grafting process was repeated up to three times.

For comparison, an MCM-41 sample with Ti incorporated in the silica framework (denoted as Ti−MCM-41) was prepared following the procedures described in refs 57 and 58. The weight percent of Ti was comparable to that of a TiO_2/SiO_2 sample prepared with an apparent surface density of 0.2 Ti/nm^2. High-surface-area bulk anatase (99.7%, Aldrich) was used as a TiO_2 reference.

The BET surface area of all samples was measured by N_2 physisorption using an Autosorb-1 (Quantachrome). The weight loading of Ti in all samples was determined by Galbraith Laboratories using inductively coupled plasma (ICP) analysis. The apparent surface density of Ti, expressed in Ti atoms per nm^2, was then calculated from the Ti loading and the BET surface area. The structure of the deposited titania was characterized by Raman spectroscopy using a Hololab Series 5000 spectrometer (Kaiser Optical) equipped with a 532 nm Nd:YAG laser operated at a power of 25 mW. Prior to acquiring the Raman spectrum, the sample was heated at 4 K/min to 773 K in 20% O_2/He (UHP) and held at this temperature for 1 h.

Diffuse reflectance UV−vis spectra were recorded using a Harrick Scientific diffuse reflectance attachment (DRP) with a reaction chamber (DRA-2CR) and a Varian-Cary 6000i spectrophotometer. Prior to acquisition of the UV−vis spectra, samples were pretreated in a flow of 20% O_2/He and heated at 4 K/min to 723 K and then held at this temperature for 1 h. Spectra were recorded at room temperature with 1−5 eV incident light. Conversion of reflectance data into absorption spectra was performed on the basis of reference reflectance of MgO using the Kubelka−Munk function ($F(R_\infty)$). Absorption edge energies were obtained as the intercept with the abscissa from a linear regression of $[(F(R_\infty))h\nu]^{1/2}$ data plotted versus $h\nu$. Temperature-programmed reaction (TPRx) of methanol oxidation was carried out using about 25 mg of TiO_2/SiO_2 (2.8 Ti/nm^2) placed in a 1/4-in OD quartz tubular reactor. The reaction temperature was measured with a thermocouple placed inside the catalyst bed, and a calibrated quadrupole mass spectrometer (Cirrus, MKS Instruments) was used for online gas analysis. The measurement procedure is described in detail in ref 11. As a pretreatment, the sample was heated in 60 cm^3/min of 20% O_2/He at a rate of 4 K/min to 773 K and then held at this temperature for 1 h. The reaction mixture was composed of 6% CH_3OH/7.5% O_2/He. The flow rate was adjusted so that the condition of 1.4 cm^3 CH_3OH/min per Ti atom was maintained.

Temperature-programmed reduction (TPR) profiles of selected samples were performed in the same apparatus as that used for methanol TPRx. Reduction was carried out in 10% H_2/He (UHP) flowing at 30 cm^3/min. The sample was heated at a rate of 10 K/min starting from 323 to 1073 K, while the concentrations of H_2 (mass 2) and H_2O (mass 18) were followed by mass spectrometry.

Reduction−Reoxidation Measurements. Reduction−reoxidation measurements were carried out in the apparatus described above using about 50 mg of sample. For the sample with the lowest Ti weight loadings [TiO_2/SiO_2 (0.2 Ti/nm^2) and Ti−MCM-41], the sample weight was increased to 100 mg, but the residence time was held constant by doubling the flow rate. Prior to sample reduction, all samples were oxidized following the procedure described above (20% O_2/He, 4 K/min to 773 K, hold for 1 h) to ensure complete oxidation and removal of surface contaminants. The reduction was then carried out in 10% H_2/He flowing at 60 cm^3/min while the temperature was increased at 4 K/min from room temperature to 923 K. The final temperature of 923 K was kept for 1 h, after which the sample was cooled in helium to the desired reoxidation temperature.

During pulsed reoxidation, the sample was constantly purged with 30 cm^3/min UHP helium. A flow of 10% O_2/He was passed through a pulse valve (VICI Valco Instruments), containing a pulse loop with a volume of 0.5 cm^3, which was heated to 393 K. One pulse was dosed to the sample every 4 min by switching the pulse valve.

Assuming standard pressure and using the ideal gas law, each oxygen pulse was expected to contain 1.5 μmol of O_2. Due to possible changes in temperature and pressure in the gas lines or differences in the exact concentration in the gas in the manifold, the exact amount of oxygen per pulse was determined by dosing three oxygen pulses through the reactor bypass and into the mass spectrometer. The mass spectrometer signal was integrated to determine the concentration of O_2 in each pulse. The actual amount of O_2 per pulse varied between 1.4 and 1.8 μmol. Each pulse reoxidation experiment was carried out until at least three pulses of equal height were measured with the mass spectrometer, indicating that no further oxygen uptake occurred.

TABLE 1: Ti Weight Loading, BET Surface Area (single point), and Average Pore Radius of Samples Used in This Study

sample	Ti loading (nm^{-2})	BET surface area ($m^2\ g^{-1}$)	av. pore radius (Å)
2.8 Ti/SiO_2	2.8	923	10
2.6 Ti/SiO_2	2.6	782	11
1.9 Ti/SiO_2	1.9	809	11
1.5 Ti/SiO_2	1.5	825	11
0.9 Ti/SiO_2	0.9	1018	10
0.2 Ti/SiO_2	0.2	1396	10
Ti−MCM-41	0.13[a]	1100	10.8
anatase	10[b]	100 (58.0[c])	8.2[c]

[a] Estimated under the assumption of 100% exposed Ti atoms. [b] Estimated from geometry of anatase(101) surface. [c] Measured after reduction−reoxidation treatment.

EPR Spectroscopy. X-band EPR measurements were performed on a Varian E-Line Century spectrometer equipped with a single microwave cavity operating at a frequency of 9.250 ± 0.0005 GHz. Samples were cooled to near 12 K using liquid He. A microwave power of 25 μW was chosen so that measurements were conducted under the condition that the intensity for all observed signals varied linearly with the square root of the power to ensure that no signal was saturated. Except for the gain, the same conditions were used for each EPR measurement. This allowed quantitative comparisons to be made among samples after all spectra were scaled to the same gain (3.2×10^3). A DPPH standard was used to determine g values.

Samples were pretreated inside the EPR tubes. To mimic the reaction experiments, a 1/16-in OD stainless steel tube was inserted just above the sample to bring the flowing gas into contact with the sample. On both the upstream and the downstream sides, the EPR tube could be isolated with two ball valves. After oxidizing the sample according to the procedure described above (20% O_2/He, 4 K/min to 773 K, held 1 h) and purging the reactor with helium, one of the following pretreatment procedures was carried out:

(1) reduction in 10% H_2/He flowing at 60 cm^3/min while the sample was heated at 4 K/min to 923 K and then held at this temperature for 1 h,

(2) heating in He flowing at 60 cm^3/min while the sample was heated at 4 K/min to 923 K and then held at this temperature for 1 h, or

(3) TPRx in 6% CH_3OH/7.5% O_2/He while the sample was heated at 2 K/min to 823 K. The flow rate was adjusted so that the condition of 1.4 cm^3 CH_3OH/min per Ti atom was maintained.

After each pretreatment, the EPR tube was purged with helium before the pressure in the EPR tube was reduced and the samples were sealed inside the tube by melting the glass.

Results and Discussion

Sample Characterization. The results of sample characterization by means of BET and ICP are summarized in Table 1. The samples used in this study had weight loadings of Ti of 0.2, 0.9, 1.5, 1.9, 2.6, and 2.8 Ti/nm^2. The BET surface area of MCM-48 was ~1500 m^2/g and is similar to values observed earlier.[59] With increasing loading of Ti, the BET surface area decreased from 1000 to 800 m^2/g, following a pattern reported previously.[14] The surface area of the reference anatase was also measured after a reduction and reoxidation because considerable sintering was expected during reduction at high temperature.

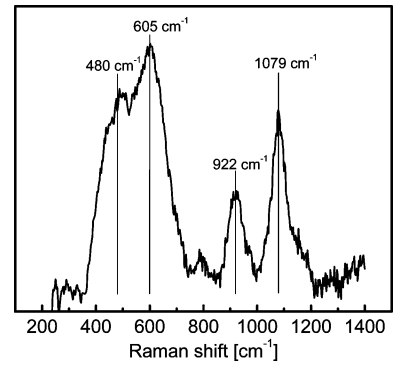

Figure 1. Raman spectrum of 2.8 TiO_2/SiO_2. The sample was heated to 773 K and then cooled under flowing UHP He before the spectrum was acquired at ambient temperature.

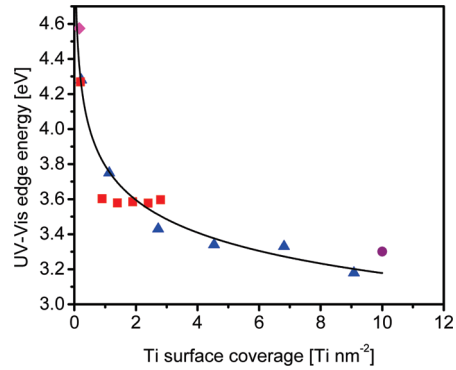

Figure 2. UV−visible edge energy as a function of the Ti surface coverage; TiO_2/MCM-48 samples (this work, red squares), Ti−MCM-41 (this work, pink diamond), TiO_2/SiO_2 (ref 15, blue triangles), TiO_2 (anatase) (this work, purple circle).

The surface area did, in fact, decrease from an initial value of 100 m^2/g to 58 m^2/g after reduction and reoxidation.

Figure 1 shows the Raman spectrum for the sample with a Ti loading of 2.8 Ti/nm^2. Similar spectra were observed for samples with lower Ti loadings but are not shown. The bands at 605 and 480 cm^{-1} can be attributed to the D1 and D2 bands of the MCM-48 support, respectively,[60] confirming that the structure of the mesoporous silica was not destroyed during the deposition of TiO_2. The Raman bands at 922 and 1079 cm^{-1} can be assigned to Si−O−Ti bonds.[3,61] The presence of these band indicates that the titania layer is bonded to the SiO_2 support. Ti−O−Ti bands would be expected in the vicinity of 460, 710, and 800−900 cm^{-1}, on the basis of previous studies of TiO_2/Al_2O_3.[62] The first two of these bands could not be observed because of the broad D1 and D2 bands for silica occurring at 605 and 480 cm^{-1}. A band was observed at 800 cm^{-1}, which may be due to Ti−O−Ti vibrations. No evidence for crystalline forms of titania was found for any of the samples, as evidenced by the absence of characteristic bands for rutile (143, 447, 612, 826 cm^{-1})[63] or anatase (146, 197, 397, 516, 640, 800 cm^{-1}).[11] The strongest of these features is the band at 145 cm^{-1}, which is a particularly sensitive detector of even very small amounts of crystalline TiO_2.[3] The absence of any features in the region of the spectrum below 200 cm^{-1} (not shown) confirms the absence of crystalline TiO_2 in the samples studied.

The edge energies obtained from the UV−vis spectroscopic measurements are shown in Figure 2 together with similar data from ref 15. The edge energies of the Ti−MCM-41 sample and the reference bulk TiO_2 (high-surface-area anatase, Aldrich) are shown for comparison. For bulk TiO_2, the number of 10 Ti surface atoms per nm^2 was estimated from geometric consid-

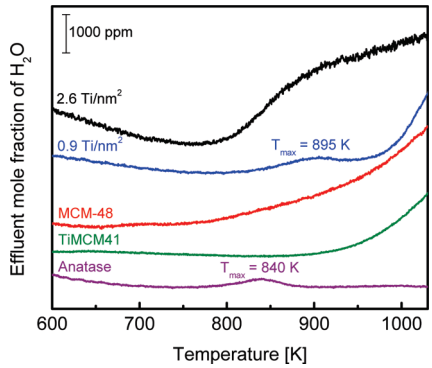

Figure 3. Mole fraction of H_2O formed during temperature-programmed reduction in 30 cm^3/min 10% H_2/He; 2.6 TiO_2/SiO_2 (black), 0.9 TiO_2/SiO_2 (blue), MCM-48 (red), Ti−MCM-41 (green), high surface area anatase (purple). The curves are shifted along the y-axis for better visibility.

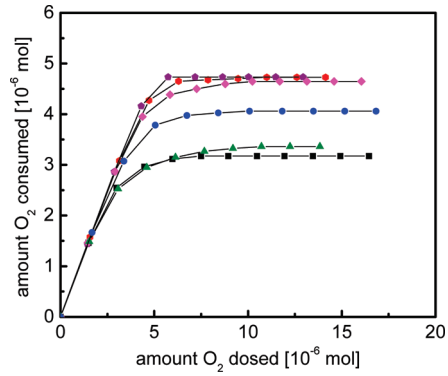

Figure 4. Uptake of oxygen during pulsed reoxidation at different temperatures for 2.8 TiO_2/SiO_2: 673 (purple), 473 (red), 423 (pink), 373 (blue), 343 (green), and 313 K (black). Lines are included in order to guide the eye.

erations of the anatase (101) surface. The decrease in the UV−visible edge energy can be attributed to an increase in the domain size of TiO_2, indicating larger "patches" or clusters of TiO_x-like structures on the surface at higher surface loading.[15,64] Values larger than 4.2 eV have been assigned to isolated, monomeric TiO_4 tetrahedra, whereas values smaller than 3.4 eV have been attributed to polymeric TiO_x-chains.[15] On the basis of the observed edge energies, only the two samples with the lowest Ti surface coverage in this study (Ti−MCM-41, and TiO_2/MCM-48 with 0.2 Ti/nm^2) clearly fall into the range of isolated TiO_4-species, whereas the samples with Ti surface densities of 0.9, 1.4, 1.9, 2.4, and 2.8 Ti/nm^2 have edge energies between those observed for isolated TiO_4 tetrahedra and polymeric chains.

The UV−visible edge energy is the same for all samples with TiO_2 surface concentrations between 0.9 and 2.8 Ti/nm^2. This observation suggests that the size of the TiO_2 domains does not increase with increasing TiO_2 surface concentration but, rather, the number of domains increases while the distance between domains decreases. This interpretation is supported by the recognition that the edge energy is obtained from the position and shape of the low wavenumber side of the UV−visible spectrum, so its value will be dominated by the properties of the largest clusters in the sample.

Sample Reduction. Three peaks for water production were observed in the TPR spectra of samples with surface concentrations of 2.6 and 0.9 Ti/nm^2 (Figure 3). The peak near 400 K (not shown in Figure 3) can be assigned to desorption of water adsorbed in the pores of the mesoporous silica.[65] The steep increase in the water signal around 1000 K was caused by condensation of silanol groups on the surface of MCM-48, accompanied very likely by a collapse of the MCM-48 structure.[65,66] This peak was absent in bulk TiO_2. For 0.9 TiO_2/SiO_2, a small peak is observed between 800 and 973 K. This peak is higher for 2.6 TiO_2/SiO_2 and coincides with the release of water via silanol condensation. This peak is absent from the TPR spectra for pure MCM-48 and Ti−MCM-41. Therefore, the peak between 800 and 973 K is assigned to partial reduction of the titania deposited on SiO_2. Since no evidence was found for the reduction of Ti−MCM-41, it is concluded that the observed water peak is due to the loss of oxygen from titania oligomers, but not from isolated titanate groups. A similar peak at 840 K was observed for high surface area anatase, in agreement with previous studies of TiO_2. The appearance of this peak at a temperature 55 K lower than that observed for TiO_2/SiO_2 indicates that the reduction of TiO_2 deposited on silica has a higher activation energy barrier than that for the reduction of anatase.

The amount of water formed by reduction of the SiO_2-supported TiO_2 was determined by integration of the peak near 900 K seen in Figure 4 after subtraction of the baseline. For the TiO_2/SiO_2 sample with 0.9 Ti/nm^2, the release of water was calculated to be 2.28 μmol H_2O, which is equivalent to 8.38 μmol O_2 per gram of sample. Assuming one molecule of H_2O is formed for each oxygen vacancy together with two reduced Ti ions, that is,[67]

$$Ti^{4+}\text{-}O\text{-}Ti^{4+} + H_2 \rightarrow Ti^{3+}\text{-}\square\text{-}Ti^{3+} + H_2O \qquad (2)$$

then 1.9% of all Ti ions in this sample should be in the 3+ state after hydrogen reduction. It is noted that in eq 2, after the removal of the oxygen atom, the former Ti−O−Ti bond is assumed to contain a vacancy. It cannot be excluded, however, that one or both of the Ti atoms are bound to OH groups which might migrate and change to a bidentate configuration, thereby increasing the coordination of the reduced Ti atoms.

We note that this measure of the extent of TiO_2 reduction may be subject to large errors caused by the sensitivity to the means by which the baseline is subtracted. Nevertheless, it is in reasonable quantitative agreement with the extent of TiO_2 reduction determined by pulse O_2 reoxidation. A similar estimate of the amount of water released upon reduction of anatase gave 1.65 μmol H_2O, equivalent to 8.21 mmolO_2/g, which using the stoichiometry of reaction 2 shows that 3.40% of all surface Ti atoms were reduced to Ti^{3+}. This value was calculated using the BET surface area measured after the reduction−reoxidation treatment and an assumed surface coverage of 10 Ti/nm^2. As will be shown below, this extent of reduction is in excellent agreement with results obtained from pulse reoxidation. Integration of the H_2O trace for the 2.6 TiO_2/SiO_2 sample was not possible because the two water peaks could not be resolved.

Pulsed Reoxidation. Plots of oxygen uptake for different reoxidation temperatures are shown in Figure 4 for the TiO_2/SiO_2 sample with 2.8 Ti/nm^2. With increasing reoxidation temperatures, a larger number of pulses is needed to reach the saturation point, and the total oxygen uptake increases. However, no changes in the total uptake were observed for temperatures above 473 K. Complete reoxidation of the sample at temperatures above 473 K was confirmed by EPR spectroscopy: when a reduced sample containing 2.8 Ti/nm^2 was reoxidized pulsewise at 473 K in the EPR tube, only a very small residual signal

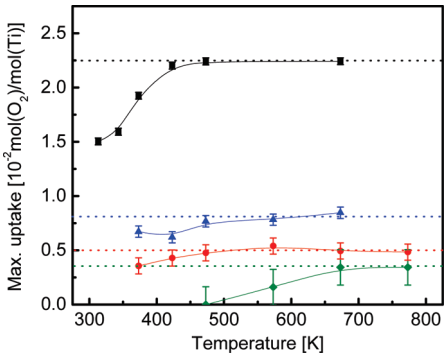

Figure 5. Maximum O_2 uptake during pulsed reoxidation as a function of temperature for 2.8 TiO_2/SiO_2 (black squares), 1.9 TiO_2/SiO_2 (blue triangles), 0.9 TiO_2/SiO_2 (red circles), 0.2 TiO_2/SiO_2 (green diamonds). Lines are included in order to guide the eye.

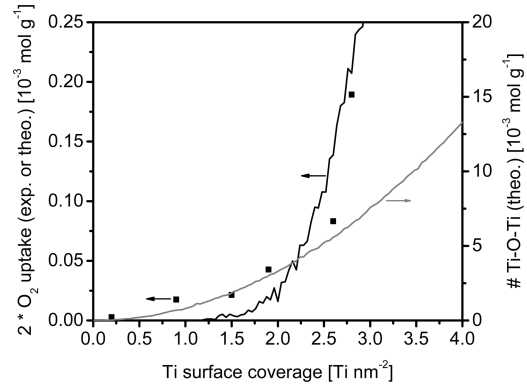

Figure 6. Comparison of the experimental O_2 uptake (black squares) with the theoretical number of Ti−O−Ti bonds (gray line) and the number of theoretically reducible Ti−O−Ti bonds for groups of eight (black line).

of the Ti^{3+} species was observed (<0.1% of all Ti atoms in the sample). The slightly incomplete reoxidation inside of the EPR tube may have been caused by the less favorable flow conditions in the EPR tube as compared with those in the reactor.

Assuming that each O_2 molecule reoxidizes four Ti^{3+} cations,[55] according to the reaction

$$2\ Ti^{3+}\text{-}\square\text{-}Ti^{3+} + O_2 \rightarrow 2Ti^{4+}\text{-}O\text{-}Ti^{4+} \qquad (3)$$

then the maximum oxygen uptake (observed for reoxidation temperatures of 473 K or above) of the TiO_2/SiO_2 sample with 2.8 Ti/nm^2 corresponds to 9.0% of all Ti cations, which were in a 3+ state prior to reoxidation. The incomplete reoxidation of the TiO_2/SiO_2 sample at temperatures below 473 K suggests that a distribution of vacancy types exits, some of which are more difficult to reoxidize than others.

Figure 5 shows the oxygen uptake per Ti atom for different TiO_2/SiO_2 samples plotted as a function of reoxidation temperature. The error bars increase with decreasing TiO_2 loading because the uptake is plotted per Ti atom. It is noted that the maximum uptake of O_2 per Ti atom decreases with decreasing TiO_2 loading. These data then show that although 9.0% of the Ti atoms can be reduced in the TiO_2/SiO_2 sample with 2.8 Ti/nm^2, only 1.4% of the Ti atoms can be reduced in the TiO_2/SiO_2 sample with 0.2 Ti/nm^2. It is also observed that the temperature required for complete reoxidation increases from 473 K for the TiO_2/SiO_2 sample with 2.8 Ti/nm^2 to 673 K for the TiO_2/SiO_2 sample with 0.2 Ti/nm^2. Complete reoxidation of the samples was confirmed in several cases by EPR spectroscopy. Consequently, the maximum uptake of oxygen measured by pulsed reoxidation is equivalent to the amount of Ti^{3+} formed upon reduction. This conclusion is further supported by the observation of the expected 2:1 ratio between the amount of H_2O formed during the TPR measurement and the amount of O_2 that was consumed during pulse reoxidation. This ratio also indicates that Ti^{3+} is not formed by a reductive removal of OH groups,

$$Ti\text{-}OH + {}^1/_2H_2 \rightarrow Ti^{3+} + H_2O \qquad (4)$$

because in this case, one H_2O would be equal to only one Ti^{3+}. The 2:1 ratio was also observed for reoxidation of anatase. The maximum uptake observed at 473 K equals 7.93 μmol O_2/g anatase, or 3.29% of all surface Ti atoms' being reducible to the 3+ state. This is in excellent agreement with the extent of reduction as observed by TPR.

Noticeable changes of the catalyst structure, such as a sintering of the TiO_x species or migration of Ti into the SiO_2 structure, do not occur during reduction or pulsed reoxidation. For all samples, repeated measurements of reduction−reoxidation showed the same uptake. If major changes to the samples had occurred during the reduction or the reoxidation process, the uptake would decrease with repeated measurements.

The change in O_2 uptake as a function of the Ti loading is likely to be an effect of the number of Ti−O−Ti bonds in the samples. Ti−O−Ti bonds are expected to lose the oxygen atom more easily than Ti−O−Si bonds, which in turn are expected to lose their oxygen bridge more easily than Si−O−Si bonds. This is due to the lower defect formation energy of TiO_2 as compared with SiO_2[24,68] and because in the case of Ti−O−Ti, the two electrons left behind on removal of the oxygen atoms can be taken up by the two neighboring Ti atoms to form two Ti^{3+}. Si atoms, in contrast, are not likely to change their oxidation state to 3+. Neither a MCM-48 sample without TiO_2 grafted on it nor the Ti−MCM-41 showed any oxygen uptake at 773 or 673 K, respectively, under the same reduction and reoxidation conditions applied to TiO_2/SiO_2 (results not shown). The absence of an EPR signal for MCM-48 and the observation of a Ti^{3+} signal hardly distinguishable from the baseline in the case of Ti−MCM-41 after both the samples had been exposed to H_2 at 923 K confirms the irreducibility of Si−O−Si and Ti−O−Si bonds. The result for Ti−MCM-41 also confirms that Ti^{3+} is not formed by reductive removal of Ti−OH, since this process could, in principle, occur for Ti−MCM-41. Consequently, the results suggest that oxygen can be removed only from Ti−O−Ti bonds.

A model of the TiO_2 layer was developed to assess whether the achievable extent of reduction scales with the number of Ti−O−Ti bonds in the samples. Ti atoms corresponding to a certain surface coverage were randomly distributed on a 100 × 100 matrix, and the expected number of Ti−O−Ti bonds was then determined as a function of coverage. Full coverage was assumed to be 4 Ti/nm^2, according to the value given in ref 3. Figure 6 shows a plot of the number of Ti−O−Ti bonds, in moles per gram, contained in the deposit (the left-hand ordinate) versus the Ti coverage in Ti atoms per square nanometer and a plot of twice the oxygen uptake in moles per gram (the right-hand ordinate) versus Ti coverage. The factor 2 is needed, because according to eq 3 one O_2 molecule reoxidizes two Ti−O−Ti bonds. As can be seen, the increase in the number

of Ti−O−Ti bonds with coverage predicted from the model agrees qualitatively with the experimental data; however, the total number of Ti−O−Ti bonds is almost 2 orders of magnitude higher than the oxygen uptake, indicating that only about 1% of all Ti−O−Ti bonds can be reduced, suggesting that the Ti−O−Ti bonds are not all equal.

It is likely that only Ti−O−Ti bonds in larger clusters of TiO_x species can be reduced because it is easier to distribute or delocalize the charges induced by the removal of the lattice oxygen atom. To test this hypothesis, the model was modified so that a Ti−O−Ti bond could be reduced only if the condition is fulfilled that both Ti atoms in this bond are fully surrounded by three more Ti−O−Ti bonds. Therefore, as soon as the central Ti−O−Ti bond is reduced, the surrounding six Ti atoms become irreducible. The results from this simulation are also plotted in Figure 6, on the right axis, on the same scale with the experimental oxygen uptake. Almost quantitative agreement is achieved for the TiO_2/MCM-48 sample with the highest weight loading of titania (2.8 Ti/nm^2), and the extremely low reducibility of the 0.2 Ti/nm^2 sample is also predicted well. However, the experimentally observed O_2 uptake during pulse reoxidation of the samples with intermediate Ti coverage (0.9, 1.5, and 1.9 Ti/nm^2) is higher than the model suggests. This might be due to a higher than expected clustering of the deposited TiO_2, resulting in part from the tendency of titanium isopropoxide to graft onto silica in the form of dimeric titania species,[69] which, in turn, could aggregate into larger than expected two-dimensional domains of titania.

The higher temperature needed for complete reoxidation of TiO_2/SiO_2 samples with lower Ti loading very likely reflects differences in the nature and spatial distribution of oxygen vacancies with TiO_2 surface density. At low TiO_2 surface densities, it is reasonable to expect that there may be only one vacancy per TiO_x patch, whereas at higher TiO_2 surface densities, each patch might be larger and may contain several oxygen vacancies, or the TiO_x patches are in closer proximity to each other. The mechanism by which vacancies are removed upon reoxidation can be envisioned to be as follows: O_2 adsorbs at a vacancy site to from an O_2^- species,[55,70] probably as shown below.

$$Ti^{3+}\text{-}\square\text{-}Ti^{3+} + O_2 \rightarrow Ti^{3+}\text{-}O_2^-\text{-}Ti^{4+} \quad (5)$$

The superoxide species thus formed then dissociates to form a Ti−O−Ti structure and a peroxide structure:

$$Ti^{3+}\text{-}O_2^-\text{-}Ti^{4+}\text{-}O^{2-}\text{-}Ti^{4+} \rightarrow Ti^{4+}\text{-}O^{2-}\text{-}Ti^{4+}\text{-}O_2^{2-}\text{-}Ti^{4+} \quad (6)$$

$$Ti^{3+}\text{-}O_2^-\text{-}Ti^{4+}\text{-}O^{2-}\text{-}Si^{4+} \rightarrow Ti^{4+}\text{-}O^{2-}\text{-}Ti^{4+}\text{-}O_2^{2-}\text{-}Si^{4+} \quad (7)$$

Reactions similar to 5 and 6 have been suggested to proceed in SiO_2,[71−74] and in the support of V/TiO_2[39] and V/SiO_2[75] catalysts. Depending on the size of the TiO_x patch and the location of the oxygen vacancy within it, the peroxide species could be located between two Ti^{4+} cations or between a Ti^{4+} cation and a Si^{4+} cation. Consumption of the peroxide species could then occur by reaction 8 or 9 when peroxide species are proximate to an oxygen vacancy; namely,

$$Ti^{4+}\text{-}O_2^{2-}\text{-}Ti^{4+}\text{-}\square\text{-}Ti^{3+} \rightarrow Ti^{4+}\text{-}O^{2-}\text{-}Ti^{4+}\text{-}O^{2-}\text{-}Ti^{4+} \quad (8)$$

$$Si^{4+}\text{-}O_2^{2-}\text{-}Ti^{4+}\text{-}\square\text{-}Ti^{3+} \rightarrow Si^{4+}\text{-}O^{2-}\text{-}Ti^{4+}\text{-}O^{2-}\text{-}Ti^{4+} \quad (9)$$

Recent theoretical studies have shown that the activation barrier for migration of peroxide species through TiO_2 is significantly lower than through SiO_2,[39,71,72,75] suggesting that peroxide migration via the reaction 5 should occur more rapidly than by reactions 6. While admittedly speculative, the proposed mechanism of peroxide formation and migration could explain the increasing ease of vacancy removal by reoxidation observed with increasing loading of TiO_2 deposited on SiO_2.

EPR Spectroscopy. After the pretreatment with 10% H_2/He at 923 K, the TiO_2/SiO_2 sample with 2.8 Ti/nm^2 was dark blue, indicating the presence of Ti^{3+} cations.[42,55] The EPR spectrum of this sample shows an intense, slightly anisotropic paramagnetic signal centered around $g = 1.932$ (Figure 7). Even though this g value is lower than typical g values reported previously for Ti^{3+} in bulk TiO_2,[17,76,77] it compares very well to g values reported for surface Ti^{3+} on TiO_2,[55,78] V/TiO_2,[79] or TiO_2 colloids.[80] This observation is reasonable, since all Ti cations are located on the surface of our sample. Subsurface or bulk TiO_2 is not present.

Figure 7 also shows the EPR spectra taken of the 2.8 Ti/nm^2 sample after it was reoxidized with O_2 pulses at different temperatures in the EPR tube. The EPR signal assigned to Ti^{3+} decreases progressively in intensity the higher the reoxidation temperature, but it does not disappear entirely at temperatures up to 373 K. This is in agreement with the incomplete reoxidation of this sample seen in Figures 5 and 6.

Apart from the paramagnetic Ti^{3+} signal, all spectra of the partially reoxidized sample showed a second paramagnetic signal centered around $g = 2.010$. This feature is absent in the fully reduced, nonreoxidized sample, so it has to be related to the presence of oxygen. The g value is in agreement with values reported for oxygen radical species such as O_2^- or O^- on TiO_2 or Ti/SiO_2,[55,81−83] but signals of those species are expected to be anisotropic and to have components of the g tensor closer to 2.00.[55,81] It is possible that some of the anisotropic components might overlap with the Ti^{3+} signal and thus be invisible. However, the O_2^- radical in particular would have the g_{zz} component with an absorbance profile at around $g = 2.025$,[55,81] which was not observed. Medium-polarized conduction electrons in reduced TiO_2 have been observed at a g value close to that of a free electron at 2.0023;[55,81] however, the amorphous TiO_x species present in the samples studied here are not likely to have a conduction band. Thus, it seems that the most reasonable assignment of the signal at $g = 2.010$ is to an O^- species.

The amount of Ti^{3+} formed upon reduction of TiO_2/SiO_2 samples can be determined by pulsed reoxidation, as was shown earlier (see Figures 5 and 6). It is, therefore, possible to correlate the strength of the EPR signal observed after sample reduction with the amount of Ti^{3+} in the sample determined by the amount of O_2 required to completely reoxidize the sample. For this purpose, it is very important to keep the EPR measurement conditions precisely the same for all measurements, including, for example, the sample volume, the shape and wall thickness of the EPR tube, the exact position of the sample in the cavity of the EPR spectrometer, and the temperature of the sample and the EPR laboratory.[84] For the measurements reported here, the sample mass was similar for all samples (17.0 ± 0.3 mg).

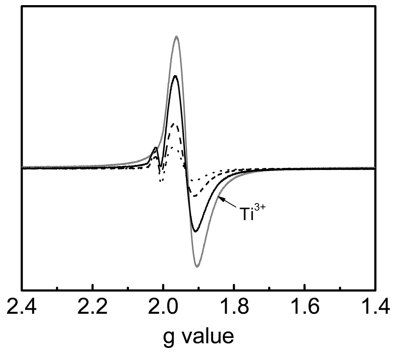

Figure 7. EPR spectra of 2.8 TiO_2/SiO_2 reoxidized with O_2 pulses at different temperatures in comparison with the spectrum of a fully reduced sample (gray); reoxidation temperature: 313 (black, solid), 343 (black, dashed), and 373 K (black, dotted).

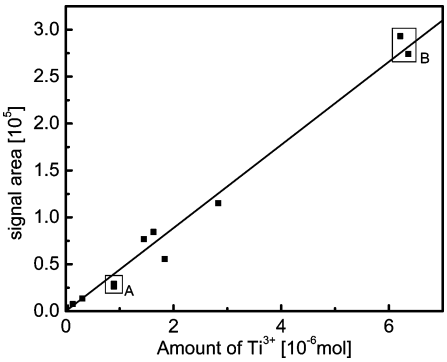

Figure 8. Correlation of signal area obtained from double integration of the Ti^{3+} signal to the amount of Ti^{3+}, as determined from pulsed reoxidation; 2.8 TiO_2/SiO_2 and 1.9 TiO_2/SiO_2 samples reoxidized at different temperatures used to generate the curve. Rectangle A: 2.8 TiO_2/SiO_2 sample, reoxidized at 343 K, two measurements, after removing and reinserting sample from the cavity. Rectangle B: 2.8 TiO_2/SiO_2 sample, fully reduced, two measurements of two samples pretreated in exactly the same way.

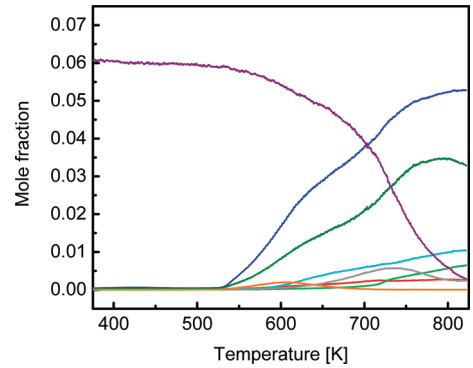

Figure 9. Temperature-programmed reaction profiles of 2.8 TiO_2/SiO_2, displaying the concentrations of CH_3OH (purple), H_2O (blue), formaldehyde (dark green), CO (cyan), CO_2 (bright green), H_2 (red), DME (gray) and MF (orange). Reaction conditions: 6% CH_3OH/7.5% O_2/He, 1.4 CH_3OH cm^3 min^{-1} per Ti atom, temperature ramp 2 K/min from 363 to 823 K.

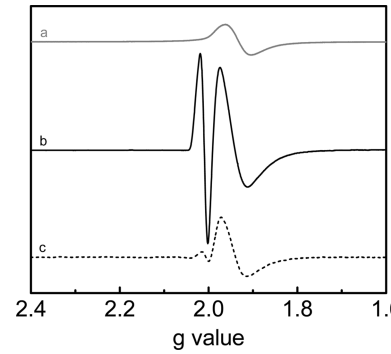

Figure 10. EPR spectra of 2.8 TiO_2/SiO_2 after different pretreatments: (a) after reduction (10% H_2/He, 4 K/min to 923 K, hold 1 h), intensity divided by factor 100; (b) after methanol oxidation TPRx (6% CH_3OH/7.5% O_2/He, 2 K/min to 823 K, then rapid cooling in He); (c) after heating in He (4 K/min to 923 K, hold 1 h).

Due to similar packing densities of the different samples, the volume of each sample was virtually the same. The EPR tubes used are similar in shape and originate from the same package (WILMAD labglass, 707-SQ-250M). The sample was positioned inside the cavity with the sample center as close as possible to the cavity center, which is the recommended position for quantitative EPR spectroscopy.[84] Spectra for all samples were measured on the same day in an air-conditioned laboratory, so the ambient conditions in the lab are assumed to be virtually the same for all samples. The sample temperature was adjusted to 12 ± 2 K.

The spectra obtained under the conditions described above were integrated twice (the first integration being necessary to account for the differential plot of EPR spectra), and the signal area can be correlated to the amount of Ti^{3+} in the sample. The correlation thus obtained is presented in Figure 8. It should be noted that the amount of Ti^{3+} was determined by reoxidation of the same sample at the same temperature in the flow reactor. Due to the numerous sources of error that have been identified for quantitative EPR spectroscopy,[84] the data points in Figure 8 display a fairly large scatter, but it is obvious that a linear correlation between Ti^{3+} amount and signal area is obtained, with a correlation factor of $R^2 = 0.984$.

Two measurements were conducted to test the reproducibility of both the EPR measurements and the sample preparation. The 2.8 Ti/nm^2 sample reoxidized at 343 K was measured twice, the second time after removing it from the cavity and reinserting it. Both points are marked with the rectangle A in Figure 8 and they almost coincide with each other, indicating the high accuracy of the EPR spectroscopic measurement. Furthermore, two reduced samples with 2.8 Ti/nm^2 were identically prepared in different tubes, and the results with these two samples are marked by rectangle B in Figure 8. Even though the difference between these two points is larger (the difference in the amount of Ti^{3+} in these samples is caused by a slightly different sample mass), the results indicate that the sample pretreatment method leads to generally consistent data.

Temperature-Programmed Oxidation of Methanol. The temperature-programmed oxidation of methanol was performed to study the state of reduction of the TiO_2/SiO_2 sample with 2.8 Ti/nm^2 under reaction conditions relevant for the catalytic process. Figure 9 shows the products formed during the oxidation of methanol on TiO_2/SiO_2 (2.8 Ti/nm^2) by temperature-programmed reaction. The principal product observed is formaldehyde. Some dimethyl ether (DME) and methyl formate (MF) are also produced, and at higher temperatures, decomposition of methanol to CO and H_2 occurs, and some CO_2 is formed. The results are in agreement with reaction data reported in ref 3. As is expected from the absence of crystalline TiO_2 in all samples, DME is not formed in large quantities.[3,11]

The correlation presented in Figure 8 can be used to estimate the amount of Ti^{3+} in differently pretreated samples with an unknown extent of reduction. Figure 10, curve b shows the EPR spectrum of the 2.8 Ti/nm^2 sample after it had undergone methanol oxidation in a temperature-programmed reaction

experiment under conditions comparable to those used to obtain the data shown in Figure 9. After 823 K was reached, the sample was purged with He and cooled to room temperature rapidly, before the pressure in the tube was reduced and the tube was sealed. This spectrum is compared with that obtained after reduction of the same sample of TiO_2/SiO_2 with H_2 (Figure 10, curve a). Note that the intensity of the spectrum of the sample acquired after H_2 reduction was divided by a factor of 100 to facilitate displaying on the same scale as that used for the sample taken after TPRx. The spectrum taken after TPRx exhibits both the paramagnetic signal of Ti^{3+} and the signal at $g = 2.010$. The amount of Ti^{3+} after TPRx is estimated by double integration of the Ti^{3+} signal and comparison of the area obtained with the correlation curve. By this means, it was established that ~0.22% of the Ti in this sample is present as Ti^{3+} after reaction.

It is possible that the reduction of TiO_2 observed after methanol oxidation in TPRx was caused when the sample was purged in He after reaction. Figure 10, curve c displays the EPR spectrum of the 2.8 Ti/nm^2 sample after it had been heated in He to 923 K and held at that temperature for 1 h, a higher temperature and much longer time than those used for purging after TPRx. The high-temperature pretreatment of the sample in He resulted in a Ti^{3+} signal equivalent to 0.04% of the Ti in the sample, which is significantly less than that observed after TPRx. Thus, it is concluded that the level of TiO_2 reduction observed after methanol oxidation by TPRx is representative of the state of the catalyst at the highest reaction temperature.

Conclusions

Submonolayer deposits of TiO_2 have been prepared on mesoporous silica (MCM-48) by grafting. Raman spectroscopy shows that the deposited TiO_2 is bonded to the silica, where as UV−visible and Raman spectroscopy suggest that the titania deposit is present in the form of two-dimensional clusters that exhibit an increasing number of Ti−O−Ti bonds with increasing Ti surface coverage. The deposited TiO_2 undergoes reduction in H_2 at temperatures near 900 K via the reaction Ti^{4+}-O-Ti^{4+} + H_2 → Ti^{3+}-□-Ti^{3+} + H_2O. The extent of reduction can be determined by the amount of water formed during H_2 reduction and by the amount of O_2 required to reoxidize the vacancies formed. The presence of surface Ti^{3+} cations formed upon reduction of TiO_2/SiO_2 is detected by the appearance of an EPR signal at $g = 1.932$. This feature disappears completely upon sample reoxidation. The maximum extent of reduction depends on the Ti loading, a larger amount of oxygen being removed the higher the Ti surface coverage. It is also found that the temperature needed to fully reoxidize the titania deposit increases with decreasing titania coverage. A linear relationship was determined between the Ti^{3+} EPR signal and the extent of reduction of the deposited titania. Using this relationship, it was established that a small fraction of the Ti atoms in deposited titania remain as Ti^{3+} during the oxidation of methanol.

Acknowledgment. This work was supported by the Director, Office of Energy Research, Office of Basic Energy Sciences, Chemical Science Division, of the U.S. Department of Energy under Contract No. DE-AC03-76SF00098. The authors thank Junko Yano and Henning Schroeder for assistance in acquiring the EPR data. Helpful advice on the interpretation of the EPR spectra was provided by one of the referees of this work.

References and Notes

(1) Diebold, U. *Surf. Sci. Rep.* **2003**, *48*, 53.
(2) Sheldon, R. A. *J. Mol. Catal.* **1980**, *7*, 107.
(3) Gao, X.; Bare, S. R.; Fierro, J. G. L.; Banares, M. A.; Wachs, I. E. *J. Phys. Chem. B* **1998**, *102*, 5653.
(4) Bandyopadhyay, M.; Korsak, O.; van den Berg, M. W. E.; Grünert, W.; Birkner, A.; Li, W.; Schüth, F.; Gies, H. *Microporous Mesoporous Mater.* **2006**, *89*, 158.
(5) Bickley, R. I.; Gonzalez-Carreno, T.; Lees, J. S.; Palmisano, L.; Tilley, R. J. D. *J. Solid State Chem.* **1991**, *92*, 178.
(6) Xie, B.; Huang, H.; Xie, Y. *Mater. Sci. Eng., B* **1999**, *57*, 150.
(7) Srinivasan, S.; Datye, A. K.; Smith, M. H.; Peden, C. H. F. *J. Catal.* **1994**, *145*, 565.
(8) Galan-Fereres, M.; Mariscal, R.; Alemany, L. J.; Fierro, J. L. G.; Anderson, J. A. *J. Chem. Soc. Faraday Trans.* **1994**, *90*, 3711.
(9) Capel-Sanchez, M. C.; Blanco-Brieva, G.; Campos-Martin, J. M.; de Frutos, M. P.; Wen, W.; Rodriguez, J. A.; Fierro, J. L. G. *Langmuir* **2009**, *25*, 7148.
(10) Cozzolino, M.; Di Serio, M.; Tesser, R.; Santecesaria, E. *Appl. Catal., A* **2007**, *325*, 256.
(11) Bronkema, J. L.; Leo, D. C.; Bell, A. T. *J. Phys. Chem. C* **2007**, *111*, 14530.
(12) Lee, E. L.; Wachs, I. E. *J. Phys. Chem. C* **2008**, *112*, 20418.
(13) Shee, D.; Deo, G. *Catal. Lett.* **2008**, *124*, 340.
(14) Vining, W.; Goodrow, A.; Strunk, J.; Bell, A. T. *J. Catal.* **2010**, *270*, 163.
(15) Ross-Medgaarden, E. I.; Wachs, I. E.; Knowles, W. V.; Burrows, A.; Kiely, C. J.; Wong, M. S. *J. Am. Chem. Soc.* **2009**, *131*, 680.
(16) Li, M.; Hebenstreit, W.; Diebold, U.; Tyryshkin, A. M.; Bowman, M. K.; Dunham, G. G.; Henderson, M. A. *J. Phys. Chem. B* **2000**, *104*, 4944.
(17) Iyengar, R. D.; Codell, M.; Karra, J. S.; Turkevich, J. *J. Am. Chem. Soc.* **1966**, *88*, 5055.
(18) Göpel, W.; Rocker, G.; Feierabend, R. *Phys. Rev. B* **1983**, *28*, 3427.
(19) Aono, M.; Hasiguti, H. H. *Phys, Rev. B* **1993**, *48*, 12406.
(20) Henrich, V. E. *Prog. Surf. Sci.* **1979**, *9*, 143.
(21) Andersson, S.; Collén, B.; Kuylenstierna, U.; Magnéli, A. *Acta Chem. Scand.* **1957**, *11*, 1641.
(22) Lu, G.; Linsebigler, A.; Yates, J. T., Jr. *J. Phys. Chem.* **1994**, *98*, 11733.
(23) Yang, S.; Halliburton, L. E.; Manivannan, A.; Bunton, P. H.; Baker, D. B.; Klemm, M.; Horn, S.; Fujishima, A. *Appl. Phys. Lett.* **2009**, *94*, 162114.
(24) Ganduglia-Pirovano, M. V.; Hofmann, A.; Sauer, J. *Surf. Sci. Rep.* **2007**, *62*, 219.
(25) Pacchioni, G. *Chem. Phys. Chem.* **2003**, *4*, 1041.
(26) Knözinger, H. *Science* **2000**, *287*, 1407.
(27) Balachandran, U.; Eror, N. G. *J. Mater. Sci.* **1988**, *23*, 2676.
(28) Idriss, H.; Kim, K. S.; Barteau, M. A. *Surf. Sci.* **1992**, *262*, 113.
(29) Thompson, T. L.; Diwald, O.; Yates, J. T., Jr. *J. Phys. Chem. B* **2003**, *107*, 11700.
(30) Kato, K.; Torii, Y.; Taoda, H.; Kato, T.; Butsugan, Y.; Niihara, K. *J. Mater. Sci. Lett.* **1996**, *15*, 913.
(31) Indrakanti, V. P.; Schobert, H. H.; Kubicki, J. D. *Energy Fuels* **2009**, *23*, 5247.
(32) Schaub, R.; Thostrup, P.; Lopez, N.; Lægsgaard, E.; Stensgaard, I.; Nørskov, J. K.; Besenbacher, F. *Phys. Rev. Lett.* **2001**, *87*, 266104.
(33) Zhang, Z.; Bondarchuk, O.; White, J. M.; Kay, B. D.; Dohnálek, Z. *J. Am. Chem. Soc.* **2006**, *128*, 4198.
(34) Laursen, S.; Linic, S. *J. Phys. Chem. C* **2009**, *113*, 6689.
(35) Pillay, D.; Wang, Y.; Hwang, G. S. *Catal. Today* **2005**, *105*, 78.
(36) Han, Y.; Liu, C.-J.; Ge, Q. *J. Phys. Chem. C* **2007**, *111*, 16397.
(37) Carrettin, S.; Hao, Y.; Aguilar-Guerrero, V.; Gates, B. C.; Trasobares, S.; Calvino, J. J.; Corma, A. *Chem.—Eur. J.* **2007**, *13*, 7771.
(38) Rodriguez, J. A.; Liu, P.; Wang, X.; Wen, W.; Hanson, J.; Hrbek, J.; Pérez, M.; Evans, J. *Catal. Today* **2009**, *143*, 45.
(39) Goodrow, A.; Bell, A. T. *J. Phys. Chem. C* **2008**, *112*, 13204.
(40) Sengupta, G.; Chatterjee, R. N.; Maity, G. C.; Ansari, B. J.; Satyanarayna, C. V. V. *J. Colloid Interface Sci.* **1995**, *170*, 215.
(41) Jug, K.; Nair, N. N.; Bredow, T. *Phys. Chem. Chem. Phys.* **2005**, *7*, 2616.
(42) Pan, J.-M.; Maschhoff, B. L.; Diebold, U.; Madey, T. E. *J. Vac. Sci. Technol. A* **1992**, *10*, 2470.
(43) Henderson, M. A. *Surf. Sci.* **1996**, *355*, 151.
(44) Henderson, M. A.; Otero-Tapia, S.; Castro, M. E. *Faraday Discuss.* **1999**, *114*, 313.
(45) Diebold, U.; Anderson, M. F.; Ng, K. O.; Vanderbilt, D. *Phys. Rev. Lett.* **1996**, *77*, 1322.
(46) Diebold, U.; Lehman, J.; Mahmoud, T.; Kuhn, M.; Leonardelli, G.; Hebenstreit, W.; Schmid, M.; Varga, P. *Surf. Sci.* **1998**, *411*, 137.
(47) Epling, W. S.; Peden, C. H. F.; Henderson, M. A.; Diebold, U. *Surf. Sci.* **1998**, *333*, 412.
(48) Marucco, J.-F.; Gautron, J.; Lemasson, P. *J. Phys. Chem. Solids* **1981**, *42*, 363.
(49) Plugaru, R. *Thin Solid Films* **2008**, *516*, 8179.

(50) Sekiya, T.; Yagisawa, T.; Kurita, S. *J. Ceram. Soc. Jpn.* **2001**, *109*, 672.
(51) Li, H.; Ma, H. T.; Li, X. Z.; Li, Z. W.; Wu, M.; Bao, X. H. *Chemosphere* **2003**, *50*, 39.
(52) Lindan, P. J. D.; Harrison, N. M.; Gillan, M. J.; White, J. A. *Phys. Rev. B* **1997**, *55*, 15919.
(53) Paxton, A. T.; Thiên-Nga, L. *Phys. Rev. B* **1998**, *57*, 1579.
(54) Hauf, C.; Kniep, R.; Pfaff, G. *J. Mater. Sci.* **1999**, *34*, 1287.
(55) Carter, E.; Carley, A. F.; Murphy, D. M. *J. Phys. Chem. C* **2007**, *111*, 10630.
(56) Bronkema, J. L.; Bell, A. T. *J. Phys. Chem. C* **2007**, *111*, 420.
(57) Uphade, B. S.; Yamada, Y.; Akita, T.; Nakamura, T.; Haruta, M. *App. Catal., A* **2001**, *215*, 137.
(58) Koyano, K. A.; Tatsumi, T. *Microporous Mater.* **1997**, *10*, 259.
(59) Morey, M. S.; Davidson, A.; Stucky, G. D. *J. Porous Mater.* **1998**, *5*, 195.
(60) Morrow, B. A.; *Spectroscopic Characterization of Heterogeneous Catalysts*; Elsevier: New York, NY, 1990.
(61) Gao, X. T.; Wachs, I. E. *Catal. Today* **1999**, *51*, 233.
(62) Vuurman, M. A.; Wachs, I. E. *J. Phys. Chem.* **1992**, *96*, 5008.
(63) Katiyar, R. S.; Krishnan, R. S. *Phys. Lett. A* **1967**, *25*, 525.
(64) Fernandez-Garcia, M. *Catal. Rev.* **2002**, *44*, 1.
(65) Chen, C.-Y.; Li, H.-X.; Davis, M. E. *Microporous Mater.* **1993**, *2*, 17.
(66) Landmesser, H.; Kosslick, H.; Storek, W.; Fricke, R. *Solid State Ionics* **1997**, *101*−*103*, 271.
(67) Khader, M. M.; Kheiri, F.M.-N.; El-Anadouli, B. E.; Ateya, B. G. *J. Phys. Chem.* **1993**, *97*, 6074.
(68) Pacchioni, G. *Solid State Sci.* **2000**, *2*, 161.
(69) Bouh, A. O.; Rice, G. L.; Scott, S. L. *J. Am. Chem. Soc.* **1999**, *121*, 7201.
(70) Green, J.; Carter, E.; Murphy, D. M. *Chem. Phys. Lett.* **2009**, *477*, 340.
(71) Hamann, D. R. *Phys. Rev. Lett.* **1998**, *81*, 3447.
(72) Ng, K. O.; Vanderbilt, D. *Phys. Rev. B* **1999**, *59*, 10132.
(73) Skuja, L.; Güttler, B. *Phys. Rev. Lett.* **1996**, *77*, 2093.
(74) Tatsumura, K.; Shimura, T.; Mishima, E.; Kawamura, K.; Yamasaki, D.; Yamamoto, H.; Watanabe, T.; Umeno, M.; Ohdomari, I. *Phys. Rev. B* **2005**, *72*, 045205.
(75) Goodrow, A.; Bell, A. T. *J. Phys. Chem. C* **2007**, *111*, 14753.
(76) Cornaz, P. F.; van Hooff, J. H. C.; Pluijm, F. J.; Schuit, G. C. A. *Discussions Faraday Soc.* **1966**, *41*, 290.
(77) Serwicka, E. *Colloids Surf.* **1985**, *13*, 287.
(78) Hurum, D. C.; Gray, K. A.; Rajh, T.; Thurnauer, M. C. *J. Phys. Chem. B* **2005**, *109*, 977.
(79) Dinse, A.; Ozarowski, A.; Hess, C.; Schomäcker, R.; Dinse, K.-P. *J. Phys. Chem. C* **2008**, *112*, 17664.
(80) Howe, R. F.; Grätzel, M. *J. Phys. Chem.* **1985**, *89*, 4495.
(81) Naccache, C.; Meriaudeau, P.; Che, M.; Tench, A. J. *Trans. Faraday Soc.* **1971**, *67*, 506.
(82) Dohshi, S.; Anpo, M.; Okuda, S.; Kojima, T. *Top. Catal.* **2005**, *35*, 327.
(83) Shvets, V. A.; Kazansky, V. B. *J. Catal.* **1972**, *25*, 123.
(84) Mazur, M. *Anal. Chim. Acta* **2006**, *561*, 1.

JP100104D